T Cell Costimulation with Anti-CD137 Monoclonal Antibodies Is Mediated by K63 – Polyubiquitin-Dependent Signals from Endosomes

Ivan Martinez-Forero, Arantza Azpilikueta, Elixabet Bolaños-Mateo, Estanislao Nistal-Villan, Asis Palazon, Alvaro Teijeira, Gema Perez-Chacon, Aizea Morales-Kastresana, Oihana Murillo, Maria Jure-Kunkel, Juan M. Zapata and Ignacio Melero

J Immunol 2013; 190:6694-6706; Prepublished online 20 May 2013;
doi: 10.4049/jimmunol.1203010
http://www.jimmunol.org/content/190/12/6694

The Journal of Immunology is published twice each month by
The American Association of Immunologists, Inc.,
9650 Rockville Pike, Bethesda, MD 20814-3994.

Print ISSN: 0022-1767 Online ISSN: 1550-6606.

T Cell Costimulation with Anti-CD137 Monoclonal Antibodies Is Mediated by K63–Polyubiquitin-Dependent Signals from Endosomes

Ivan Martinez-Forero,*,† Arantza Azpilikueta,* Elixabet Bolaños-Mateo,* Estanislao Nistal-Villan,* Asis Palazon,* Alvaro Teijeira,* Gema Perez-Chacon,‡ Aizea Morales-Kastresana,* Oihana Murillo,* Maria Jure-Kunkel,§ Juan M. Zapata,‡,1 and Ignacio Melero*,¶,1

Agonist anti-CD137 (4-1BB) mAbs enhance CD8-mediated antitumor immunity. Agonist anti-human CD137 mAbs binding to four distinct epitopes on the CD137 glycoprotein costimulated T cell activation irrespective of the engaged epitope or its interference with CD137L binding. CD137 perturbation with all these agonist mAbs resulted in Ag and Ab internalization toward an endosomal vesicular compartment. Internalization was observed in activated T lymphocytes from humans and mice, not only in culture but also in Ab-injected living animals. These in vivo experiments were carried out upon systemic i.v. injections with anti-CD137 mAbs and showed CD137 internalization in tumor-infiltrating lymphocytes and in activated human T cells transferred to immunodeficient mice. Efficient CD137 internalization required K63 polyubiquitination and endocytosed CD137-containing vesicles recruited TNFR-associated factor (TRAF) 2 and were decorated with K63 polyubiquitins. CD137 stimulation activates NF-κB through a K63-linked polyubiquitination-dependent route, and CD137-associated TRAF2 becomes K63 polyubiquitinated. Consistent with a role for TRAF2 in CD137 signaling, transgenic mice functionally deficient in TRAF2 showed delayed immunotherapeutic activity of anti-CD137 mAbs. As a whole, these findings advance our knowledge of the mechanisms of action of anti-CD137 immunostimulatory mAbs such as those currently undergoing clinical trials in cancer patients. ***The Journal of Immunology*****, 2013, 190: 6694–6706.**

CD137 (4-1BB/TNFRSF9) was described by Kwon and Weissman (1) as a surface activation marker of T lymphocytes. Stimulation of CD137 with agonist Abs or its natural ligand costimulates Ag-primed T cells to survive, proliferate, and develop effector functions (2). Moreover, stimulation of CD137 has been shown to be involved in the development of $CD8^+$ T cell memory and reversal of anergy (3). CD137 expression is not restricted to T cells and can be found on activated NK cells, dendritic cells, B cells, mastocytes, and myeloid precursors (4–7). Ectopic expression of CD137 has been documented on vascular cells in tumor capillaries and atherosclerotic lesions (8–10).

CD137 stimulation in tumor-bearing mice elicits a potent, often curative, immune response mediated mainly by CTL (11). Such activity can be synergistically combined with other immunotherapeutic approaches (vaccines, other immunostimulatory mAbs, and adoptive T cell therapy), as well as with radio- or chemotherapy (12–16). Clinical trials are being implemented in cancer patients with two fully human IgG_4 mAbs (BMS-663513/Urelumab and PF-05082566) (17, 18).

Early signaling events downstream CD137 following stimulation of the receptor are far from clear. Protein–protein associations with TNFR-associated factor (TRAF) 2 and TRAF1 have been reported in transfectants overexpressing tagged proteins (19, 20). The group of Saoulli et al. (21) showed coprecipitation of TRAF2 alongside CD137 in activated cultures of mouse primary T cells. TRAF2 has been described to exert ubiquitin E3 ligase activity via its RING domain (22–24). This activity links a ubiquitin moiety to a target protein or C terminus of another ubiquitin through the K63 residue. K63 polyubiquitination was discovered by Chen et al. (25) and Karin and Gallagher (26) as a key mechanism in signal transduction toward the NF-κB, IFN regulatory factor, and MAPK routes. Importantly, such pathways are tightly regulated by specific deubiquitinases, for which deficiency in the mouse genome leads to inflammation and autoimmunity (27, 28).

*Centro de Investigación Médica Aplicada, Universidad de Navarra, Pamplona 31008, Spain; †Hospital Pablo Tobon Uribe, Medellin 69-240, Colombia; ‡Instituto de Investigaciones Biomedicas "Alberto Sols," Consejo Superior de Investigaciones Científicas/Universidad Autónoma de Madrid, Madrid 28049, Spain; §Bristol-Myers Squibb, Princeton, NJ 08540; and ¶Clinica Universitaria, Universidad de Navarra, Pamplona 31008, Spain

[1]J.M.Z. and I.M. share credit for senior authorship.

Received for publication October 31, 2012. Accepted for publication April 17, 2013.

This work was supported by the Ministerio de Economía y Competitividad (SAF2008-03294 and SAF2011-22831 to I.M. and SAF2011-23846 and PI12/01135 to J.M.Z.). I.M. was also supported by the Departamento de Educacion del Gobierno de Navarra and the Departamento de Salud del Gobierno de Navarra, Redes Tematicas de Investigacion Cooperativa (RD06/0020/0065), the European Commission VII Framework Programme, the Programme of Territorial Cooperation of the European Southwest Area-Immunotherapy Network, and "Union Temporal de Empresas for project Fundacion de Investigacion Médica Aplicada." I.M.-F. is supported by an Alejandro Lopez Fellowship from the World Bank-Departamento Administrativo de Ciencia, Tecnología e Innovación Colciencias. A.P. is a recipient of a Fondo de Investigaciones Sanitarias predoctoral scholarship. A.T. and A.M.-K. are recipients of predoctoral scholarships from the Ministerio de Economia. G.P.-C. is the recipient of a Junta de Ampliacion de Estudios contract from the Consejo Superior de Investigaciones Científicas.

Address correspondence and reprint requests to Prof. Ignacio Melero, Centro de Investigación Médica Aplicada, Universidad de Navarra, Avenida Pio XII, 55, 31008 Pamplona, Spain. E-mail address: imelero@unav.es

The online version of this article contains supplemental material.

Abbreviations used in this article: EBSS, Earle's Balanced Salt Solution; EEA1, early endosome Ag-1; HA, hemagglutinin; KO, knockout; RT, room temperature; tg, transgenic; TRAF, TNFR-associated factor; *Traf*2DN, TNFR-associated factor 2 deletion mutant lacking the RING and zinc finger domains; WGA, wheat germ agglutinin; WT, wild-type.

www.jimmunol.org/cgi/doi/10.4049/jimmunol.1203010

In this study, we show that agonist anti-CD137 mAbs trigger CD137 internalization to an endosomal compartment both in vitro and in vivo, and we provide genetic and biochemical evidence showing that CD137 signals via K63 polyubiquitination to activate NF-κB.

Materials and Methods

Mice

BALB/c wild-type (WT) mice (5 to 6 wk old) were purchased from Harlan Laboratories. Rag2($^{-/-}$)IL-2Rγ($^{-/-}$) and OT-I TCR-transgenic (tg) mice were purchased from The Jackson Laboratory and bred in our animal facility under specific pathogen-free conditions. CD137 knockout (KO) mice (BALB/c background) were generated at Lexicon Genetics. TRAF2 deletion mutant lacking the RING and zinc finger domains (*Traf*2DN)-tg mice were previously described (29) and have been bred into a BALB/c background. Animal procedures were conducted under institutional guidelines that comply with national laws and policies (study 066/10).

Cell lines and transfections

CT26, CEM, and HEK293T cells were obtained and authenticated from American Type Culture Collection. Cells were cultured in complete RPMI medium (RPMI 1640 with Glutamax [Life Technologies, Invitrogen] containing 10% heat-inactivated FBS [Sigma-Aldrich], 100 IU/ml penicillin, and 100 μg/ml streptomycin [Life Technologies]). Culture medium for mouse cell lines was supplemented with 50 μM 2-ME (Life Technologies).

To generate HEK293T-CD137-GFP cells, DNA encoding human CD137 with GFP (pCMV6-CD137-GFP; Genecopia) in the cytoplasmic end was transfected using Lipofectamine 2000 (Invitrogen) according to the manufacturer's instructions, followed by selection with G418 (400 μg/ml; Life Technologies). Fluorescent cells were enriched by two rounds of sterile FACS sorting (FACSAria II).

Hybridoma production

C57BL/6 female mice (6–8 wk old) were i.p. immunized at days 0, 15, 30, and 45 with 10 μg recombinant human CD137 protein and IFA. For hybridoma production, splenocytes from immunized mice were fused with NSO myeloma cells at a ratio of 3:1 and distributed in 96-well plates (Costar, Cambridge, MA). Screening of mAb reaction with human CD137 was performed by indirect immunofluorescence and flow cytometry (FACScan; BD Biosciences, San Jose, CA). The mAbs were purified by affinity chromatography in HiTrap Protein G HP columns (GE Healthcare), according to the manufacturer's instructions.

T cell costimulation

Human PBMCs were obtained from buffy coats provided by the blood bank of Navarra, Spain, after written informed consent (Ethics Committee from the University Clinic of Navarra 007/2007 and 013/2009). Human CD3 mAb (OKT3) was precoated overnight in six-well plates at 2 μg/ml. PBMCs were labeled with 0.25 μM CFSE (Sigma-Aldrich) and then cultured for 7 d with 10 μg/ml anti-CD137 mAb or control mouse Ab. CFSE cell content was assessed by FACS every day during the culture period. Harvesting and activation of OT-1 splenocytes with synthetic SIINFEKL peptide (5 μg/ml) was performed as described (30).

CD137 internalization in vitro and in vivo

Activation of CEM T cells was performed by incubation with PMA (0.1 μg/ml)–ionomycin (1 μg/ml) for 18 h. Human primary lymphocytes were induced to express CD137 by culturing them in anti-CD3ε mAb–coated (2 μg/ml) 24-well plates for 48 h. HEK293T transfectants or activated T cells were then stimulated with 10 μg/ml biotinylated anti-CD137 (clone 6B4). Cross-linking was induced when indicated with 10 μg/ml Alexa 594-streptavidin. After the indicated time, cells were fixed, permeabilized, and stained with Alexa 488 wheat germ agglutinin (WGA) and DRAQ5. Images were obtained with an LSM 510 Zeiss confocal microscope using a 40× or 63× oil immersion objective (Zeiss, Welwyn Garden City, U.K.).

For in vivo experiments, Rag2$^{-/-}$γR$^{-/-}$ double KO mice were inoculated with 1×10^6 activated CEM or human T cells i.p. and then were injected i.v. with 100 μg anti-CD137 (clone 6B4) or control mouse IgG Ab. After 2 h, cells were extracted via peritoneal lavage and stained as described above.

CD137 surface expression was quantified at the indicated time points by FACS. CD137 expressing HEK293T or activated CEM cells were stimulated for 10 min at 4°C with 10 μg/ml nonlabeled human anti-CD137 (6B4 or 5D1) or isotype control. After washing two times with PBS, cells were incubated during 10 min with biotin rat anti-mouse IgG_1 (5 μg/ml) at 4°C. Then, cells were cultured in RPMI 1640 for 15, 30, or 60 min at 37°C. Afterwards, cells were treated with 0.4 ng/ml allophycocyanin-streptavidin at 4°C during 10 min, washed two times in PBS, fixed in 2% paraformaldehyde during 10 min, and analyzed using an FACS Calibur instrument (BD Biosciences).

Experiments with the rest of the human anti-CD137 mAbs in Supplemental Fig. 1 were performed with similar results.

The percentage of cells containing anti-CD137 endosomes was quantified in Figs. 2D and 3D. For each experiment, a total of 30 cells was analyzed per field in three different fields of confocal microscopy images.

To detect early endosome Ag-1 (EEA1) and CD137 codistribution, HEK293T (7×10^6) were transfected with 2.25 μg CD137 plasmid. After 16 h, cells were stimulated with 5 μg/ml biotin-labeled human anti-CD137 (clone 6B4) for 10 min at 4°C and then washed twice in PBS. Cross-linking was induced with 10 μg/ml Alexa 488-streptavidin. HEK293T cells were then cultured at 37°C for the indicated time (0 or 30 min), fixed with 4% paraformaldehyde during 15 min at 4°C, and then permeabilized with 0.1% Triton X-100 in PBS for 15 min. Cells were incubated during 30 min with four drops of Image iT FX signal enhancer (Invitrogen) to avoid nonspecific binding, and samples were blocked using Earle's Balanced Salt Solution (EBSS) containing 10% BSA, 0.1% Triton X-100, and 0.1% saponin for 1 h. EEA1 was detected with a rabbit polyclonal Ab (Abcam) diluted in EBSS 0.1% Triton X-100, 0.1% saponin, and 1% BSA. After three washes, cells were labeled with 10 μg/ml Alexa 647 anti-rabbit Ab (Invitrogen) for 1 h. Then, samples were embedded in 0.8% agar (Sigma-Aldrich), and images were obtained with an LSM 510 Zeiss confocal microscope using a 40× or 63× oil immersion objective (Zeiss).

Transfection and reporter assays

Transient transfection of HEK293T cells was performed using Lipofectamine 2000 (Invitrogen) according to the manufacturer's instructions. Cells were transfected with 200 ng pκB-Luc plasmid, which encodes a firefly luciferase reporter gene under the control of an NF-κB–responsive promoter (31) and with 200 ng constitutive expression plasmid Renilla luciferase reporter vector pRL-TK (Promega), as well as with h*cd137* (Origene), TRAF2-GST (150 ng; Addgene Plasmid 21586; Addgene) (32), TRAF2ΔRING (up to 500 ng), pcDNA-flag-TRAF2ΔRING (33) (a kind gift from Dr. Adrian Ting, Mount Sinai School of Medicine), pcDNA 3.1$^+$-hemagglutinin (HA)-ubiquitin (up to 500 ng), and pcDNA 3.1$^+$-HA-ubiquitin K63R (up to 500 ng) (both a kind gift from Gijs Versteeg, Mount Sinai School of Medicine). Twelve to 18 h after transfection, cells were harvested and lysed in dual reporter lysis buffer (Promega). Firefly luciferase values were normalized using Renilla luciferase values. When indicated, cells were stimulated for 6 h with 10 μg/ml anti-CD137 mAb (clone 6B4) and then lysed in dual reporter luciferase buffer (Promega).

For luciferase reporter experiments in lymphoid cell lines, 25×10^6 CEM or MOLT4 cells per condition were electroporated using the Gene Pulser MX System (300 V for CEM, 250 V for MOLT4, 950 μF for both cell types; Bio-Rad, Hercules, CA) with plasmids encoding CD137 (10 μg), K63R (20 μg), κB-firefly luciferase reporter (10 μg), pRL-TK (10 μg), or empty vector (20–30 μg). After 24 h, live cells were isolated using Ficoll density gradient separation, washed, and stimulated during 16 h with 10 μg/ml anti-CD137 mAb (clone 6B4) or control Ab (Mouse IgG; Sigma-Aldrich).

CD137 ubiquitin K63 colocalization in vivo and in vitro

Tumor-infiltrating lymphocytes were obtained from CT26 tumors s.c. implanted in the flank of BALB/c mice. At day 12 after tumor implantation, mice were treated i.v. with 100 μg mouse biotinylated anti-CD137 mAb (clone 17B5) or isotype control. Two hours following treatment, tumors were excised and subjected to mechanical dissociation and Ficoll (Lympholyte-M; Cedarlane Laboratories, Burlington, NC) separation to isolate infiltrating T lymphocytes.

For in vitro experiments, CEM or primary lymphocytes were activated as previously described. CD137 stimulation was accomplished with 10 μg/ml biotinylated anti-CD137 (clone 6B4). Cross-linking was induced with 1 μg/ml Alexa 488-streptavidin.

After stimulation, cells were fixed with 4% paraformaldehyde during 15 min at 4°C and then permeabilized with 0.1% Triton X-100 in PBS for 5 min. To avoid nonspecific binding, all samples were blocked using EBSS containing 10% BSA, 0.1% Triton X-100, and 0.1% saponin for 1 h. Cells were stained overnight with an Ab recognizing ubiquitin K63-specific

chains diluted in EBSS containing 1% BSA, 0.1% Triton X-100, and 0.1% saponin (1:40; clone Apu3; Millipore) (34). Samples were washed three times with 0.1% Triton X-100 in PBS and incubated with 200 μl Image-IT Fx signal enhancer (Invitrogen) for 15 min at room temperature (RT). After three washes, cells were labeled with 10 μg/ml Alexa 647 anti-rabbit Ab (Invitrogen) for 1 h. Then, samples were embedded in 0.8% agar (Sigma-Aldrich). Images were obtained with an LSM 510 Zeiss confocal microscope using a 40× or 63× oil immersion objectives (Zeiss). At least 30 cells were evaluated per condition.

For colocalization analyses, threshold over background was set, and a region of interest was manually defined around individual cells. Colocalization was measured with the coloc_2 module of FIJI (35).

Colocalization of CD137, TRAF2, and K63-ubiquitin was analyzed in HEK293T (7×10^6) cells transfected with CD137 in pReceiver-M02 (2.25 μg) (GeneCopoeia, Germantown, MD) and pcDNA3 HA-TRAF2 (2.25 μg) for 16 h. Cells were stimulated, and cross-linking was induced as previously described with biotinylated human anti-CD137 Ab (clone 6B4) and Alexa 488-streptavidin. Cells were fixed (4% paraformaldehyde) and permeabilized (0.1% Triton X-100 in PBS) as described before. TRAF2 was stained with rat anti-HA mAb (1:400; clone 3F10; Roche, overnight at 4°C). Endogenous K63–polyubiquitin chains were detected with clone Apu3 (1:40; Millipore, overnight at 4°C). After extensive washing, cells were labeled with 10 μg/ml Alexa 647 anti-rabbit Ab (Invitrogen) and Alexa 546 anti-rat Ab (Invitrogen) for 1 h. For confocal imaging, samples were embedded in 0.8% agar (Sigma-Aldrich). Images were acquired with an LSM 510 Zeiss confocal microscope using a 40× or 63× oil immersion objective (Zeiss). Triple codistribution was quantified using a custom-developed FIJI plugin that defines a mask in the green channel and then detects the colocalization percentage of blue and red channels inside the mask. It also allows calculation of the corrected Pearson correlation inside the green mask.

NF-κB nuclear translocation

To determine the presence of p65 NF-κB in HEK293T nuclei, cells were seeded on glass culture slides (BD Falcon 8-well CultureSlide; BD Biosciences), grown to 80% confluence, and stimulated for 30 min with anti-CD137 (clone 6B4) at a concentration of 1 μg/ml. Afterwards, cells were fixed in 4% formaldehyde for 10 min at RT, permeabilized, blocked with goat serum for 30 min at RT, and then incubated with anti-p65NFκB1 primary Ab (Santa Cruz Biotechnology) overnight. Secondary goat anti-rabbit (DakoCytomation) was incubated for 45 min at RT. Samples were mounted in SlowFade Antifade Kit (Invitrogen) and evaluated by using a epifluorescence microscope Zeiss AxioImager (Zeiss) and ISIS software (Metasystems, Altlussheim, Germany).

p65 NF-κB nuclear translocation was also evaluated by immunoblot. Briefly, HEK293T were transfected with plasmids encoding CD137, TRAF2ΔRING, and K63R-ubiquitin for 16–18 h and then nuclear extracts obtained using the Qproteome Cell Compartment Kit (Qiagen).

Immunoblots were performed with Abs against p65 (rabbit polyclonal; Santa Cruz Biotechnology) and Lamin A/C (clone 636; Santa Cruz

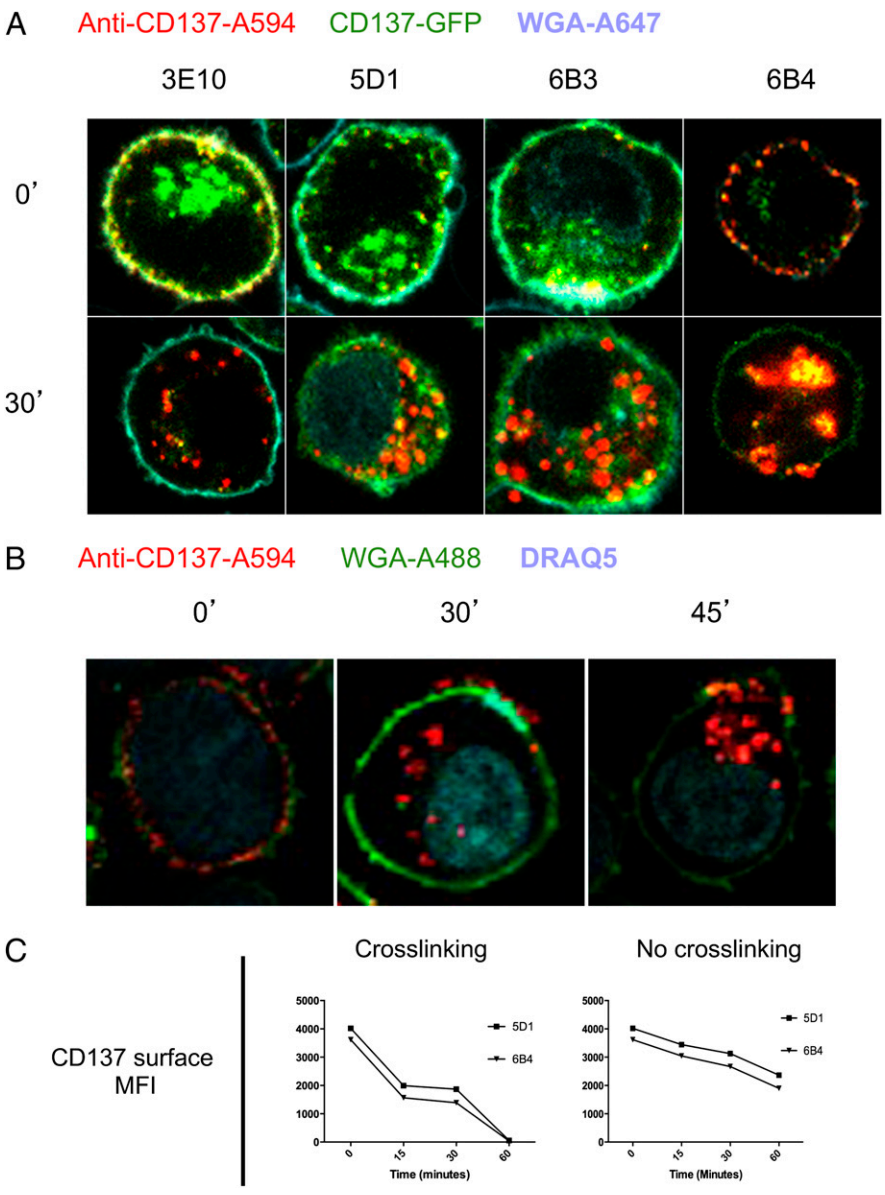

FIGURE 1. CD137 internalization upon ligation with anti-CD137 agonist mAbs. (**A**) HEK293T cells stably expressing human CD137-GFP were stimulated with the different anti-CD137 Abs described in Supplemental Fig. 1. Cells were fixed immediately after anti-CD137 mAbs conjugated with Alexa 594 were added (time 0) or 30 min later (time 30 min). Samples were analyzed by confocal microscopy (original magnification ×40). (**B**) CEM cells (human T cell line) were activated with 0.1 μg/ml PMA-1 μg/ml ionomycin for 18 h. Cells were fixed and then incubated with biotin-conjugated anti-CD137 mAb (clone 6B4) for the indicated times. CD137 was detected with Alexa 594-streptavidin, and nuclei were stained with DRAQ5. Confocal images were taken with a ×40 oil immersion objective. Original magnification ×400. (**C**) CD137 cell-surface expression (mean fluorescence intensity [MFI]) was quantified at the indicated time points by FACS. HEK293T-expressing CD137 were stimulated with 6B4 or 5D1 human anti-CD137 mAbs. Cross-linking was induced with biotin rat anti-mouse IgG_1. Remaining CD137 surface expression was detected with allophycocyanin-streptavidin.

Biotechnology). Blots were developed with the ECL Western Blotting Substrate (Pierce). Densitometry was performed with the Gel Tool from FIJI.

Immunoprecipitation

HEK293T cells were transfected as described above with plasmids encoding CD137, TRAF2-GST, ubiquitin-HA, K63R-ubiquitin-HA, or K48-ubiquitin HA. Sixteen hours after transfection, CD137 stimulation was accomplished with 10 μg/ml anti-CD137 (clone 6B4). Cross-linking was induced with 10 μg/ml purified anti-mouse IgG_1 (eBioscience). Then cells were lysed at 4˚C in lysis buffer (25 mM Tris-HCl [pH 7.5], 150 mM NaCl, 1% Nonidet P-40, 1 mM EDTA, and complete protease inhibitor [Roche]). Soluble lysate was immunoprecipitated with 5 μg anti-CD137 mAb (clone 6B4) and 80 μl protein G-Sepharose 4 Fast Flow beads (GE Healthcare) or with glutathione Sepharose beads for TRAF-GST pulldown. Proteins were eluted in Laemmli sample buffer two times with 2-ME, separated by SDS-PAGE, and transferred to polyvinylidene difluoride membranes. Membranes were blocked in PBS containing 0.05% Tween-20 and 5% nonfat milk for 1 h. Immunoblots were performed with Abs against CD137 (clone 6B4), HA (rabbit polyclonal; Abcam), or GST (rabbit polyclonal; Sigma-Aldrich). Blots were developed with the SuperSignal West Dura Extended Duration Substrate (Pierce). Densitometry was performed with the Gel Tool from FIJI.

In vivo NF-κB reporter assay

CD137 KO mice (BALB/c) at 6–8 wk of age (8) were anesthetized using ketamine/xylazine and then were injected with a total amount of 20 μg plasmid DNA by hydrodynamic injection, consisting of the administration of 1.8–2.0 ml DNA solution via tail vein in 5 s (36). Animals were injected with plasmids encoding a κB-firefly luciferase reporter (6 μg), CD137 (4 μg), K63R-ubiquitin (10 μg), or with an empty plasmid (empty vector) as required. At 48 h after hydrodynamic injection, mice were i.p. inoculated with 100 μg human anti-CD137 mAb (clone 6B4) or control mouse IgG.

Bioluminescence measurement

Mice were anesthetized using ketamine/xylazine and injected with 100 μl D-luciferine (Xenogen, Alameda, CA) at a concentration of 30 mg/ml. Mice were placed in the imaging chamber of the Xenogen IVIS system (Xenogen). A color-scale photograph of the animals was acquired, followed by a bioluminescent acquisition. Regions of interest were drawn over the positions of greatest signal intensity on the animal, as well as over regions of no signal, which were used as background readings. Light intensity was quantified using photons/s/cm^2/sr (luciferase activity). The color-scale photograph and data images from all studies were superimposed using LivingImage (Xenogen).

Western blotting in Traf2DN-tg mice T cells

Spleens from 3–6-mo-old *Traf2*DN-tg mice and WT littermates were mechanically processed, and mononuclear cells were isolated by Ficoll density centrifugation (Lympholyte-M; Cedarlane Laboratories). T cells were purified from spleens of mice using the EasySep negative selection mouse T cell enrichment kit (Stem Cell Technologies, Vancouver, Canada) following the manufacturer's instructions. Purity of T cells was assessed by FACS using anti–CD3-FITC mAb and was >95%. T cells (4×10^6 cell/sample) were lysed, sonicated and protein concentration was determined. A total of 12 μg protein from each sample was analyzed by SDS-PAGE/immunoblotting using specific Abs against TRAF2, TRAF5 (Santa Cruz Biotechnology), p52 NF-κB (Cell Signaling Technologies, Danvers, MA), and β-actin (Sigma-Aldrich).

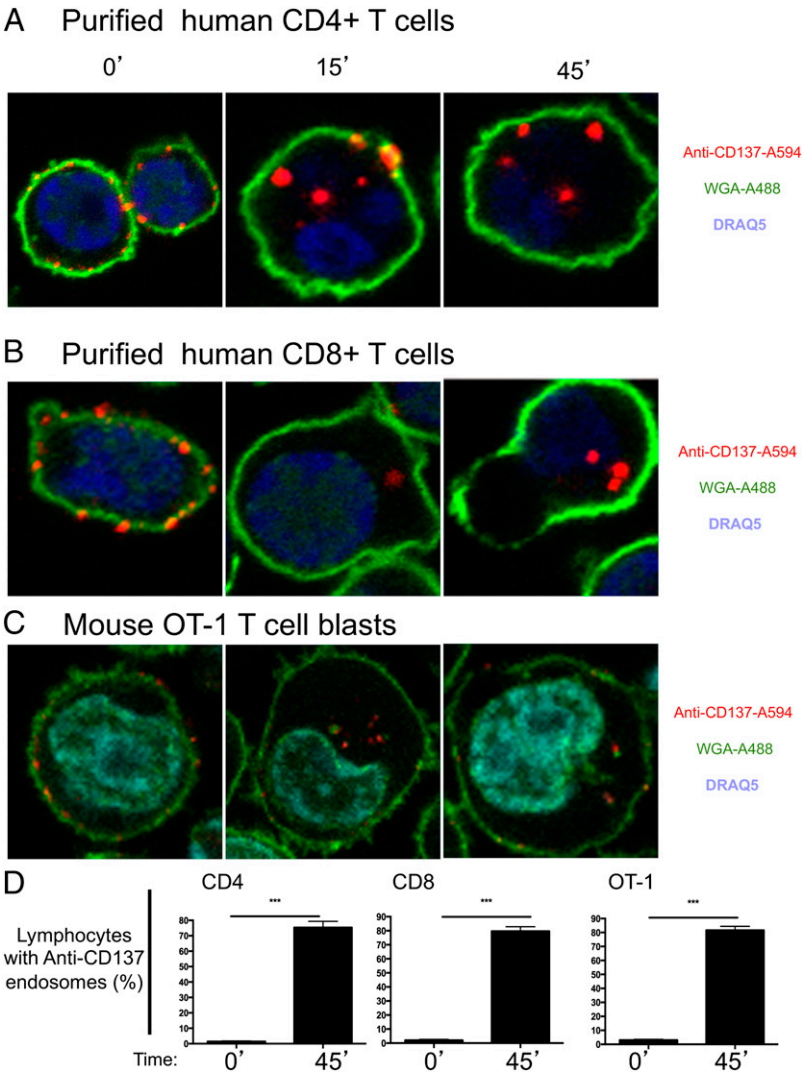

FIGURE 2. CD137 is internalized upon ligation with anti-CD137 agonist mAbs in primary human and mouse T cells. Immunomagnetically purified human CD4 (**A**) or human CD8 T (**B**) cells were activated with anti-CD3 mAb to induce CD137 expression. After 24 h, cells were stimulated with Alexa Fluor 594–conjugated human anti-CD137 mAb (clone 6B4) for the indicated times. Samples were analyzed by confocal microscopy with a 40× oil immersion objective. Similar results were observed with the other anti-CD137 mAb of the panel (not shown) (**C**). Splenocytes derived from OT-1 TCR-tg mice were stimulated with SIINFEKL OVA peptide for 48 h. Cells were stimulated for the indicated times with biotinylated anti-mouse CD137 (clone 17B5) and cross-linked with streptavidin-Alexa Fluor 594. WGA-A488 was used to counterstain the plasma membrane in green. Cells were fixed, and samples were analyzed by confocal microscopy with a 40× oil immersion objective. Nuclei were stained with DRAQ5. For (A)–(C), original magnification ×400. (**D**) The percentages of cells containing at least one anti-CD137–containing endosome were quantified at the indicated time points. For each experiment, a total of 30 cells was analyzed per field in three different fields of confocal microscopy images. ***$p < 0.0001$.

Tumor immunotherapy experiments

*Traf*2DN-tg mice and WT littermates (6–8 wk old) bred into a BALB/c background were subdermally inoculated with 5×10^5 mouse colon carcinoma CT26 cells resuspended in 100 μl PBS. One week later, mice (n = 8/genotype and treatment) were i.p. injected either with 100 μg 1D8 anti-CD137 mAb or isotype control and the treatment was repeated 3 and 6 d later. Tumor length and width was measured with an electronic digital caliper every 2 d, and tumor volume was calculated with the formula $V = \pi/6 \times \text{length} \times \text{width}^2$.

Statistical analysis

Prism software (GraphPad Software) was used to analyze CD137 internalization, CD137 colocalization with K63–polyubiquitin, NF-κB–dependent luciferase expression, and tumor growth. Statistical significance between groups was assessed by applying unpaired Student t tests or two-way ANOVA tests: $^*p < 0.05$, $^{**}p < 0.01$, $^{***}p < 0.0001$.

Results

CD137 when ligated by agonist mAbs internalizes to an endosomal compartment

A panel of mouse IgG_1 mAbs directed to human CD137 was raised against a CD137-Fc chimera (Supplemental Fig. 1). All of these Abs specifically recognize human CD137 transfectants in HEK293T by immunofluorescence and FACS analyses. The panel of mAbs detected the protein in immunoblot assays and, with the exception of 6B3 mAb, was also capable of immunoprecipitating CD137 (Supplemental Fig. 1). Unfortunately, none of the mAb in our panel raised against human CD137 cross-reacted with mouse CD137 (data not shown). The five selected mAb define four epitopes, with only one of them (clone 6C10) interfering with binding of the natural CD137 ligand (CD137L) as a soluble recombinant protein. In cultures of human T cells preactivated by surface-coated anti-CD3ε mAb, all of the anti-CD137 mAbs costimulated proliferation in CFSE dilution assays and inhibited T cell death, irrespective of the engaged epitope (Supplemental Fig. 1). All of these mAbs bind CD137 with a K_D in the low nanomolar range (Supplemental Fig. 1).

HEK293T cells were stably transfected to express CD137 with a GFP tail. Confocal images from these cells in culture in the presence of the panel of red-labeled anti-CD137 mAbs showed that both Ab and surface Ag were rapidly internalized toward a vesicular endosomal compartment (Fig. 1A, Supplemental Video 1). The internalization event also took place in human CEM T cells prestimulated with PMA-ionomycin to acquire CD137 expression (Fig. 1B). Using unlabeled 6B4 or 5D1 mAb to induce CD137 internalization and a fluorochrome-labeled noncompeting anti-CD137 mAb, it was possible to observe an important decrease of CD137 on the plasma membrane of HEK293T CD137 stable transfectants (Fig. 1C). CD137 was not internalized when cells

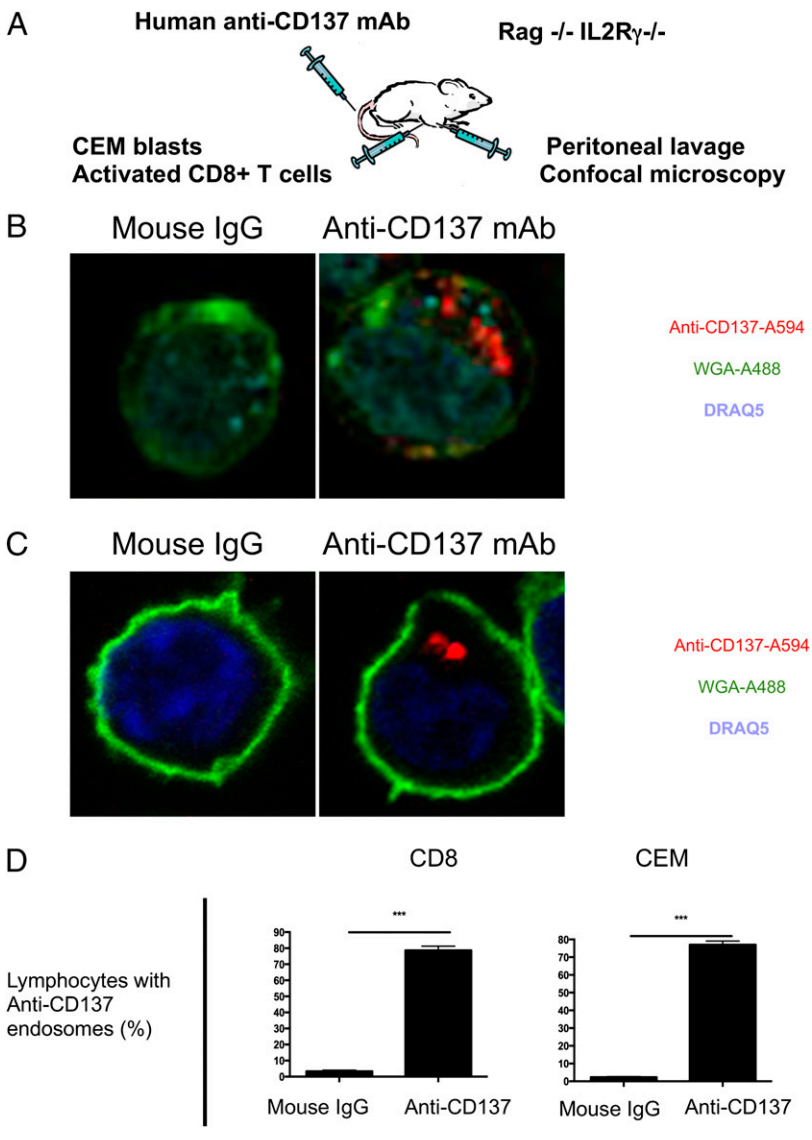

FIGURE 3. CD137 is internalized in primary T cells upon ligation by anti-CD137 agonist mAbs in vivo. (**A**) Scheme of the experiment: human CD8 T cells or CEM cells were activated to induce CD137 expression, and then 1×10^6 cells were injected in the peritoneum of $Rag^{-/-}IL\text{-}2R\gamma^{-/-}$ mice. At the same time, 100 μg human anti-CD137 mAb (clone 6B4) labeled with Alexa Fluor 594 was i.v. inoculated, and 2 h later, cells were retrieved by peritoneal lavage, fixed, permeabilized, stained, and visualized by confocal microscopy. Nuclei were counterstained with DRAQ5 and plasma membranes with Alexa 488–labeled WGA. (**B**) Confocal analysis of a representative preactivated CEM cell retrieved from the peritoneum of mice treated with control mouse IgG or with anti-human CD137 mAb. (**C**) Confocal analysis of a representative preactivated primary peripheral blood CD8 lymphoblast retrieved from the peritoneum of mice treated with mouse IgG or with anti-mouse CD137 mAb. For (B) and (C), original magnification ×400. (**D**) Quantification of cells containing endosomes with anti-CD137 mAb in preactivated primary peripheral blood CD8 lymphoblasts or preactivated CEM T cells retrieved from the peritoneum of mice treated with either mouse IgG or anti-CD137 mAb. The percentage of cells containing anti-CD137 endosomes was quantified at the indicated time points. For each experiment, a total of 30 cells was analyzed per field in three different fields of confocal microscopy images. $^{***}p < 0.0001$.

were cultured at 4°C or when treated with an isotype control mAb (data not shown). Loss of membrane immunostaining because of internalization was more rapid and efficient when cross-linking was enforced with a secondary anti-mouse IgG_1 mAb (Fig. 1C).

Primary CD4 and CD8 human T lymphocytes preincubated for 48 h with plate-bound anti-CD3ε to induce CD137 expression also showed rapid CD137 internalization upon Ab binding (Fig. 2A, 2B). This effect was not restricted to human T cells because TCR-tg OT-1 $CD8^+$ T cells prestimulated with the cognate OVA peptide Ag also experienced internalization of a red-labeled anti-mouse CD137 mAb (Fig. 2C). Internalization vesicles containing the anti-CD137 mAbs were readily observed in a majority of cultured cells (Fig. 2D). Furthermore, immunostaining experiments showed that internalized CD137 codistributed with clathrin enrichments (data not shown), thus suggesting the involvement of the clathrin internalization machinery in CD137 endocytosis. In contrast, endocytosed CD137 failed to colocalize with caveolin vesicles (data not shown). The CD137-containing vesicles were derived from the plasma membrane because a fraction of cell-surface glycoproteins prestained with the Alexa 488–labeled WGA lectin were cointernalized with CD137 toward the same vesicular compartment (Supplemental Fig. 2). In further support of the endosomal localization of internalized CD137, we found that CD137 also codistributed with the endosomal marker EEA1 (Supplemental Fig. 3).

The mechanism of action of CD137-targeted cancer immunotherapy requires that T cells recognize and get activated by tumor Ags, thus inducing CD137 expression on the surface of the best responding T lymphocytes (30). Once properly primed, these T cells become CD137 positive and responsive to artificial costimulation by an injected multivalent CD137 agonist mAb. To model such a therapeutic setting, we injected CD137-expressing PMA plus ionomycin–activated CEM human T lymphocytes in the peritoneal cavity of IL-$2R\gamma^{-/-}Rag^{-/-}$ mice and i.v. administered the agonist 6B4 anti-CD137 mAb or a control IgG (Fig. 3A). Two hours later, i.p. T cells were recovered by peritoneal lavage. Confocal microscopy of these cells clearly shows the internalization of Alexa 594–labeled 6B4 anti-CD137 mAb to endosomes (Fig. 3B). Furthermore, when primary human $CD8^+$ preactivated lymphoblasts were injected in the peritoneum of such immunodeficient mice, Alexa-conjugated 6B4 internalization was also readily observed in the activated $CD8^+$ T lymphoblasts (Fig. 3C). Similar results were observed with the rest of our anti-human CD137 mAb panel (data not shown). As a result of internalization, most lymphocytes showed CD137-containing endosomes within 45 min after injection (Fig. 3D). These results suggest that CD137 internalization takes place in vivo in situations resembling the context of CD137-targeted stimulation for immunotherapy.

Internalized CD137 codistributes with K63–polyubiquitin chains

CD137 signaling has been shown to involve TRAF2 (19–21) and TRAF1 complexes (37, 38). In fact, TRAF2 KO mice signal

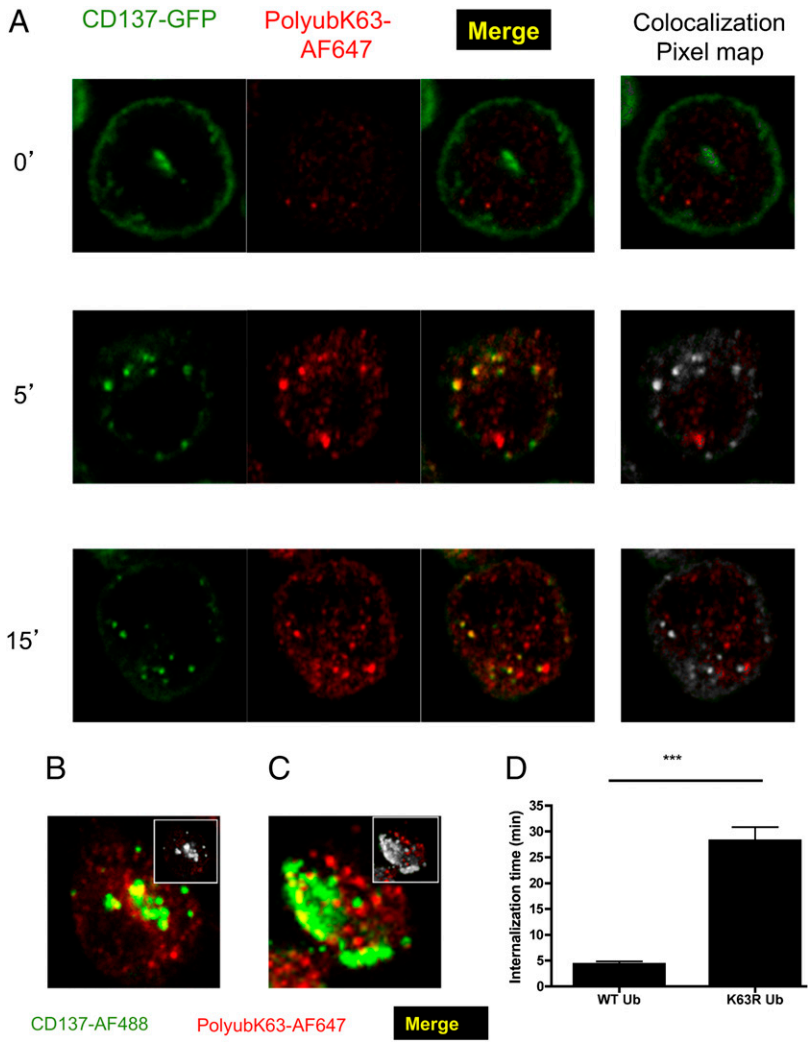

FIGURE 4. K63–polyubiquitin colocalized with CD137 and K63 polyubiquitination is required for efficient CD137 endocytosis. (**A**) HEK293T cells stably expressing CD137-GFP were stimulated with agonist 6B4 anti-CD137 (10 μg/ml) mAb for the indicated time and then fixed in 4% paraformaldehyde, permeabilized with Triton X-100, and stained with an Ab specific for K63–polyubiquitin (PolyubK63) chains (clone Apu3, 1:40). Samples were analyzed by confocal microscopy with a 40× oil immersion objective. Images are representative of two independent experiments similarly performed. Colocalization pixel maps were obtained using the coloc_2 module from FIJI. Primary human CD8 T cells (**B**) or mouse T cells isolated from the spleen of OT-1 mice (**C**) were activated with anti-CD3 mAb or cognate peptide Ag, respectively, for 48 h to induce CD137 surface expression. Cells were then stimulated with biotinylated agonist 6B4 (10 μg/ml) anti-CD137 mAb or with 17B5 biotinylated anti-mouse CD137 (10 μg/ml) cross-linked with streptavidin-Alexa Fluor 488 (10 μg/ml) (B) for 20 min and then fixed in 4% paraformaldehyde, permeabilized with Triton X-100, blocked, and stained with an Ab specific for K63–polyubiquitin chains (PolyubK63; clone Apu3, 1:40). Samples were analyzed by confocal microscopy with a 40× oil immersion objective. Cells shown are representative of the results obtained in at least three independent experiments. The *insets* in (B) and (C) represent a colocalization pixel map obtained with the coloc_2 module of FIJI. For (A)–(C), original magnification ×400. (**D**) Time to internalization after anti-CD137 mAb treatment in HEK293T-CD137-GFP cells transfected with WT or mutant K63R ubiquitin as quantified by sequential confocal microscopy. Additional information is presented as Supplemental Video 2. ***$p < 0.0001$.

poorly via CD137 (21). TRAF2 can ubiquitinate substrates with K63–polyubiquitin chains that act as docking sites for TAB2/3 adapters and lead to canonical NF-κB pathway activation via TAK1 and also to the activation of MAPKs (39, 40). No evidence of CD137 triggering ubiquitination-dependent signaling events has been ever described, but previous evidence with other TNFR members such as CD40 and TNFR1 is available (41–43).

We performed experiments of CD137 internalization on HEK293T cells stably transfected with CD137-GFP. Upon binding with the agonist mAb 6B4, CD137-GFP, and K63–polyubiquitin chains [immunostained with an anti-K63–polyubiquitin-specific rabbit mAb (34)] showed an overlapping distribution pattern involving intracellular endosomes in the majority of examined cells (Fig. 4A). These results suggest that the anti-CD137 agonist mAb and CD137 remain as an active signaling complex, thus constituting signaling endosomes.

Consistent with these results, CD137-induced K63 polyubiquitination was also detected on activated $CD8^+$ T lymphoblasts from human donors upon activation with an agonist anti-CD137 mAb. As shown in Fig. 4B, 20 min after ligation, internalized CD137 codistributed with K63–polyubiquitin chains upon staining with the mAb specific for K63–polyubiquitin chains. A similar result was achieved in mouse OT-1–tg T cells prestimulated with cognate Ag and exposed for 20 min to the fluorescence-labeled anti-mouse CD137 mAb and subsequent labeling with anti-K63–polyubiquitin mAb (Fig. 4C).

Furthermore, transfection of HEK293T cells expressing CD137-GFP with either WT or K63R ubiquitin showed that, upon ligation with agonist anti-CD137 mAb, CD137-GFP internalization was significantly delayed in cells transfected with the plasmid encoding the K63R ubiquitin mutant when compared with that of cells transfected with the plasmid encoding WT ubiquitin (Fig. 4D, Supplemental Video 2). This result indicates that CD137 endocytosis and K63 polyubiquitination are tightly linked events, similar to what has been previously described for other surface receptors. Indeed, K63-linked polyubiquitination has been associated with clathrin-dependent endocytosis of several surface receptors (44–46).

To further recapitulate the in vivo immunotherapy settings, we took advantage of the expression of CD137 in tumor-infiltrating T lymphocytes responding to colon CT26 cells transplanted onto BALB/c mice (47). As shown in Supplemental Fig. 4, i.v. injection of Alexa 594–labeled 17B5 anti-mouse CD137 mAb resulted in internalization of CD137 in tumor-infiltrating lymphocytes after 2 h, and anti-CD137 mAb-containing endosomes were costained with K63–polyubiquitin chains.

CD137-mediated NF-κB activation requires K63 polyubiquitination and is partially dependent on TRAF2

To ascertain the role of TRAF2 and K63 polyubiquitination in CD137-mediated NF-κB activation, transient transfections in HEK293T cells were performed with expression plasmids encoding CD137, a mutant TRAF2 lacking the RING and zinc finger domains (TRAF2ΔN), and an NF-κB reporter system controlling the expression of luciferase (Fig. 5A). As expected, CD137 overexpression in HEK293T cells induced NF-κB–dependent luciferase activity, which was further increased by ligation with anti-CD137 mAb. Expression of the TRAF2ΔN mutant significantly reduced NF-κB activation, which was drastically inhibited by expressing the K63R ubiquitin construct (Fig. 5A). Similar results were obtained with the human T cell lines CEM and MOLT4 (Fig. 6). The role of TRAF2 and K63-ubiquitination in CD137-mediated NF-κB activation was further demonstrated assessing the nuclear translocation of the p65 NF-κB1 subunit by cell immunostaining and immunoblotting of nuclear extracts. Indeed, CD137 expression in HEK293T cells efficiently induced p65–NF-κB1 nuclear translocation, and this translocation was significantly prevented by enforced coexpression of either TRAF2ΔN

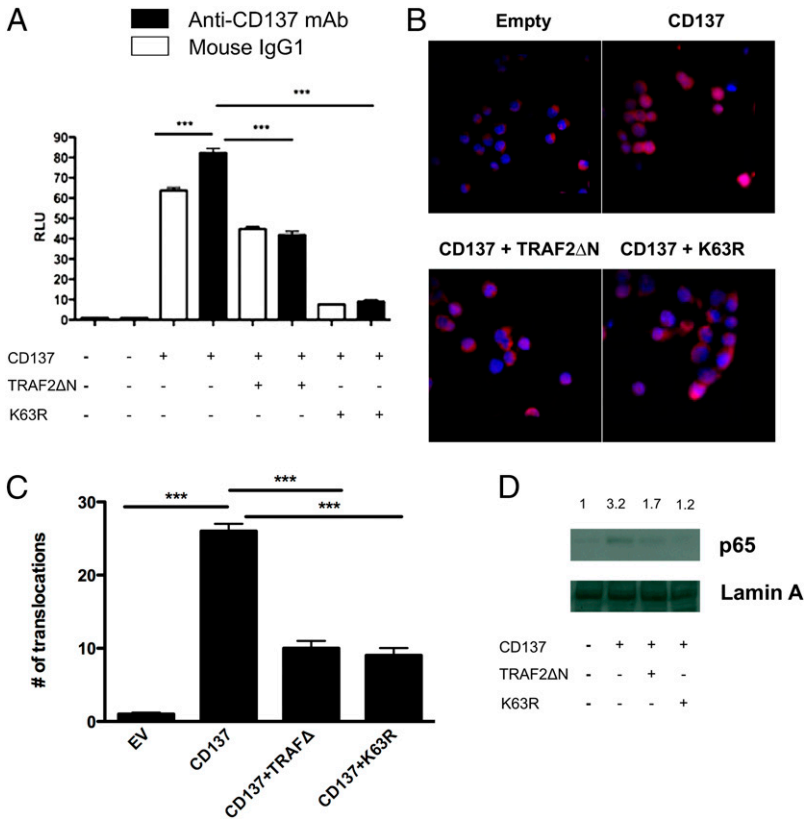

FIGURE 5. CD137 activation of NF-κB signaling is dependent on K63 polyubiquitination and TRAF2. (**A**) HEK293T cells were transfected with the indicated plasmids, and 4 h after transfection, cells were treated with anti-CD137 agonist mAb (clone 6B4) for 6 h, and luciferase expression was assessed. (**B**) HEK293T cells were transiently transfected with the indicated plasmids. After 30 min, cells were fixed, permeabilized, and stained with anti-p65–NF-κB Ab to assess its cytosolic or nuclear location. Nuclei were counterstained with DAPI. Samples were mounted in SlowFade Antifade Kit (Invitrogen) and evaluated using an epifluorescence microscope, Zeiss AxioImager (Zeiss). Original magnification ×400. (**C**) Cumulative data for the experiments displayed in (B). Data represent analysis of 30 cells/field. (**D**) Nuclear extracts from HEK293T cells transfected with CD137, TRAF2ΔRING, or K63R ubiquitin were evaluated by immunoblot for p65 NF-κB translocation. The nuclear protein lamin A used as loading control. Densitometry data are provided in each lane. ***$p < 0.0001$. EV, Empty vector.

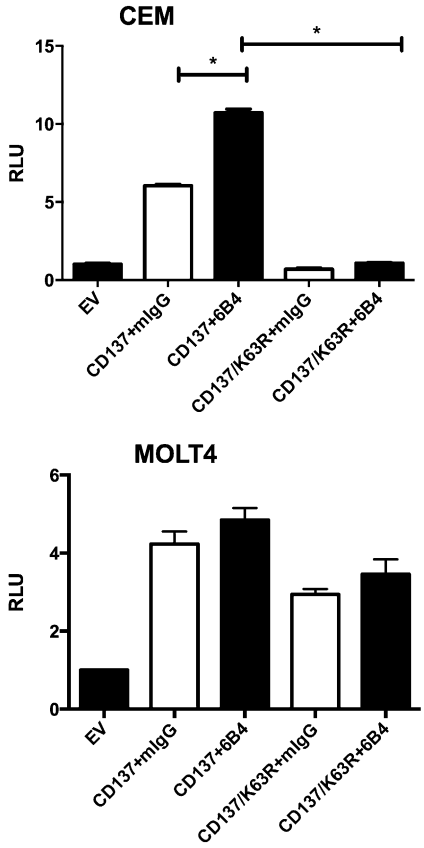

FIGURE 6. CD137 activates NF-κB in T cell lines through a K63-ubiquitin–dependent mechanism. CEM and MOLT4 cells were electroporated with plasmids encoding CD137 (10 μg), K63R (20 μg), κB-firefly luciferase reporter (10 μg), pRL-TK (10 μg), or empty vector (EV; 20–30 μg as needed to control electroporated DNA). After 24 h, live cells were isolated using Ficoll density gradient separation, washed, and stimulated with 10 μg/ml anti-CD137 mAb (clone 6B4) or control Ab (Mouse IgG). Sixteen to 18 h after Ab stimulation, cells were harvested and lysed in dual reporter lysis buffer. Firefly luciferase values were normalized using Renilla luciferase values. Experiments were done in quadruplicate. $*p < 0.05$. mIgG, Murine IgG; RLU, relative light units.

or K63R ubiquitin (Fig. 5B–D). Altogether, these data indicate that TRAF2-associated E3 ubiquitin ligase activity and K63 polyubiquitination are required for CD137-mediated NF-κB activation.

K63 polyubiquitination of TRAF2 in response to CD137 ligation

TRAF2 has been shown to interact with the cytoplasmic tail of CD137 (19). We confirmed this interaction by bidirectional coprecipitation of TRAF2-GST and human CD137 in cotransfected HEK293T cells (Fig. 7A). To study whether CD137 engagement with agonist mAbs elicits K63 polyubiquitination of TRAF2, we performed experiments in HEK293T cells, which were transfected with plasmids encoding human TRAF2-GST and HA-tagged WT, K48R, or K63R ubiquitin. Cells were then stimulated with 6B4 anti-CD137 mAb and lysed at the indicated time points. TRAF2-GST was subsequently pulled down, and the precipitates were then probed with anti-HA Abs in Western blots to detect polyubiquitinated TRAF2. As shown in Fig. 7B, an increase in HA–polyubiquitin was found covalently bound to TRAF2 as early as 2 min after CD137 stimulation. TRAF2 polyubiquitination was also observed when cells were transfected with mutant K48R ubiquitin, but this effect was completely lost upon transfection with mutant K63R ubiquitin, hence indicating that K63 polyubiquitination of TRAF2 is triggered by CD137. In addition, Fig. 8 shows that CD137, TRAF2, and K63 polyubiquitin codistributed in the signaling endosomes, hence further supporting the interplay of these molecules in the endosomal compartment.

K63 polyubiquitination is required for CD137 signaling in vivo

To ascertain the functional relevance of anti-CD137 agonist mAb in vivo, first we carried out hydrodynamic liver gene transfer of the plasmid encoding the luciferase reporter system for NF-κB activation and a combination of the aforementioned expression plasmids. NF-κB activation in mouse hepatocytes was read as luciferase-dependent light emission from the epigastric region in a luminometric chamber. As can be seen in Fig. 9A, CD137 gene transfer led to slight NF-κB–dependent light emission over control levels that was dramatically upregulated when the mice were treated i.p. with the 6B4 human anti-CD137 mAb. Importantly, gene cotransfer of plasmids encoding K63R-ubiquitin abrogated luciferase-dependent light emission (Fig. 9A, 9B), indicating that K63 ubiquitination is critical for CD137 signaling under these conditions.

TRAF2 is involved in CD137-mediated antitumor activity

As indicated earlier, CD137 stimulation in tumor-bearing mice elicits a potent, often curative, immune response mediated mainly by CTLs (11). To address the role of the CD137/TRAF2 axis in the immune rejection of tumors as elicited by agonist anti-CD137 mAb, we performed experiments in tg mice (*Traf*2DN-tg) expressing a mutant TRAF2 lacking the RING and zinc finger domains specifically in lymphocytes (29). We have recently shown in these mice that expression in B lymphocytes of TRAF2DN abrogates endogenous TRAF2 expression, thus turning *Traf*2DN-tg B lymphocytes into bona fide TRAF2-deficient lymphocytes (48). We have extended these results to *Traf*2DN-tg T lymphocytes, which also lacked significant WT TRAF2 expression (Fig. 9C). As shown in Fig. 9D, CT26 tumors that aggressively grow in both *Traf*2DN-tg and WT littermates were rejected upon treatment with anti-CD137 mAb. However, there was a significant delay (of ~1 wk) in the rejection of CT26 tumors induced by CD137 mAb treatment in *Traf*2DN-tg mice when compared with that of WT littermates. Because CD137-mediated tumor rejection was delayed but still achieved in mice functionally deficient for TRAF2, other proteins, particularly other TRAF family members such as TRAF1 (20, 37) or even TRAF5, that could substitute TRAF2 in regulating signaling from certain TNFR family members (49) might also participate in CD137-mediated tumor rejection. Of note is that both the *Traf*2DN-tg mice and WT littermates, which attained complete rejection upon treatment with anti-CD137 mAb, were able to efficiently reject a second inoculation of CT26 cells performed 2 mo later, thus indicating that TRAF2 does not seem to be required to render tumor-protective T cell memory in mice that had previously rejected a tumor upon anti-CD137 mAb therapy (data not shown).

Discussion

Immunotherapy based on agonist mAbs that engage surface receptors of the TNFR superfamily on cells of the immune system is still in its infancy in terms of clinical trials and with regard to the precise elucidation of the mechanisms of action (17, 50, 51). In this report, we have addressed the study of the early signaling events triggered by the engagement of CD137 with specific agonist mAbs that elicit a therapeutic response.

We have observed a rapid internalization of CD137 following the exposure to agonistic Abs both in vitro and, more importantly,

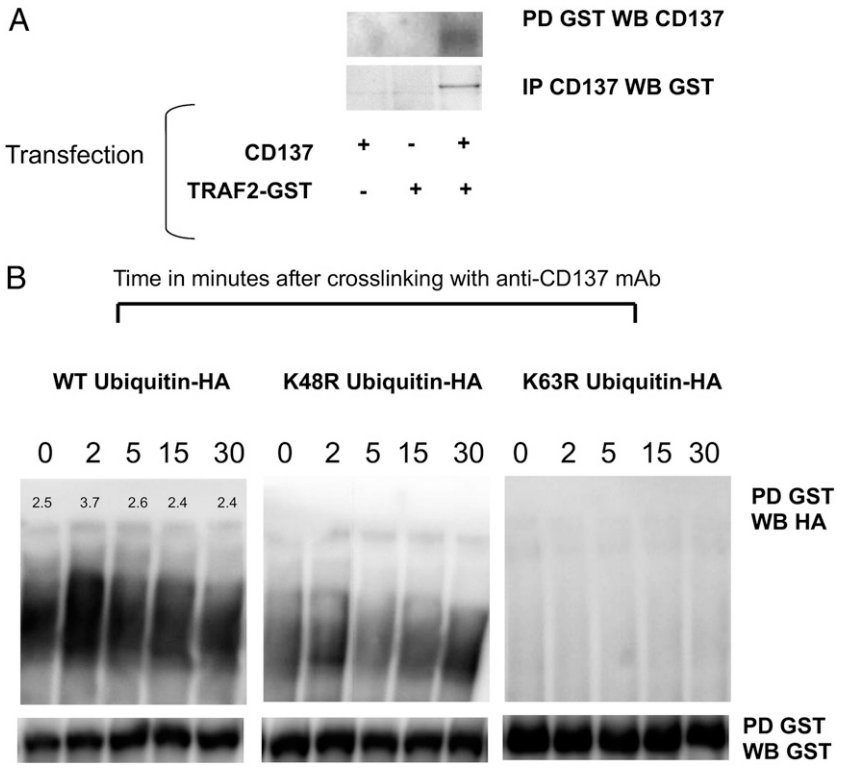

FIGURE 7. TRAF2 is ubiquitinated with K63-linked polyubiquitins following stimulation of the cells with anti-CD137 mAb. (**A**) CD137 coprecipitates with TRAF2. Lysates from HEK293T cells transiently transfected with CD137 or TRAF2-GST were precipitated with anti-CD137 mAb or glutathione-coated beads. TRAF2 or CD137 were assessed by SDS-PAGE and immunoblot using an anti-GST (rabbit polyclonal) or anti-CD137 (clone 6B4) Ab as indicated in the figure. (**B**) HEK293T cells were transfected with plasmids encoding CD137, TRAF2-GST, and HA-ubiquitin, HA-K63R–ubiquitin, or HA-K48R–ubiquitin. After 16 h, cells were treated with 6B4 anti-CD137 mAb for the indicated times. Then, cells were lysed, and GST-TRAF2 was precipitated with glutathione sepharose beads. TRAF2 ubiquitination was assessed by SDS-PAGE and immunoblot using an anti-HA Ab.

in vivo. Internalization and recycling has been observed with many surface receptors of cells of the immune system (52) but its significance for immunotherapy with immunostimulatory mAbs remains unclear. Transient disappearance of the activated receptor from the membrane would hamper rapid restimulation of the pathway until the receptor surface expression is regained. However, in the case of CD137, our results indicate that internalized CD137 molecules remain associated to the agonist cross-linking ligand, forming an endosomal depot organelle that keeps CD137-mediated signaling activated. We have previously referred to such organelles as CD137-signalsomes (53), and we postulate that they are important to understand the immunotherapeutic effects.

Furthermore, CD137 internalization in vivo upon its activation with agonist mAb would have important therapeutic consequences. First, it would preclude Ab-dependent complement activation through the classical pathway. Indeed, CD137 internalization might explain why no CD137-depleting Abs have ever been described. Second, removal of the circulating pool of anti-CD137 mAb might also prevent or, at least, delay development by the host of Abs against the immunotherapeutic CD137 mAb, a common downfall event that has been reported even for fully humanized mAb used in therapy (54).

Further research is necessary to ascertain whether the formation of such CD137-signaling endosomes in T lymphocytes might be dependent on the type and amount of the agonistic ligand available. In this regard, it remains to be elucidated whether CD137 internalization would take place when the anti-CD137 mAb or CD137L is attached to the plasma membrane of tumor cells. This is particularly relevant to therapy because it has been shown that tumor membrane-bound anti-CD137 mAbs efficiently trigger an immunotherapeutic response (55). It will be also important to assess the role of internalization upon CD137–CD137L interaction at physiological immune synapses.

The intimate mode of action of the anti-CD137 mAbs is not well understood (53). It is known that the natural ligand forms trimers that constitute the active form of the receptor (56, 57). Interestingly, five different anti-CD137 mAbs defining three separate epitopes on the molecule, including one interfering with CD137L, produce similar, if not identical, agonistic effects on CD137 signaling. These results suggest that triggering efficient signal transduction from CD137 simply requires receptor multimerization by multivalent ligands, rather than ligand-specific conformational changes in the receptor. Whether further cross-linking events of CD137 by FcR engagement acting from neighboring cells would strengthen CD137 signaling, as has been reported with anti-CD40 mAb (58, 59), is a question under investigation. The cross-linking role of FcRs could also foster internalization.

Our findings might help to understand pharmacodynamics and receptor expression/occupancy upon treatment with CD137 agonists. For instance, given our observations of in vivo internalization, it is open to debate whether it is more convenient to maintain serum levels of anti-CD137 mAb constant, or it would rather be advisable to allow CD137 surface re-expression before administering another round of treatment to the patient. In addition, the cytoplasmic tail of CD137 in tandem with those of CD3ζ and CD28 have been included in chimeric Ag receptors used in a few cases of adoptive T cell therapy with unprecedented clinical success (60, 61). Our results may provide the basis to understand early signaling events from these successful chimeric Ag receptors.

Mechanisms involving endocytosis should be expected for other TNFR superfamily members (i.e., GITR, OX40, and CD27 in T cells), and it would be important to take endocytosis into consideration when interpreting the immunotherapeutic effects elicited through the corresponding immunostimulatory mAbs (56). Internalization to endosomes of CD137 (or other relatives of the TNFR superfamily) with specific cross-linking agents could be envisioned as a tool to build endosomal pools continuously signaling inside the cell. Costimulation with CD137 in cis has been previously described in T cells cotransfected with CD137 and CD137L (62).

We have also performed in vitro studies using transfected HEK293T cells and the T cell lines CEM and MOLT4. Our results

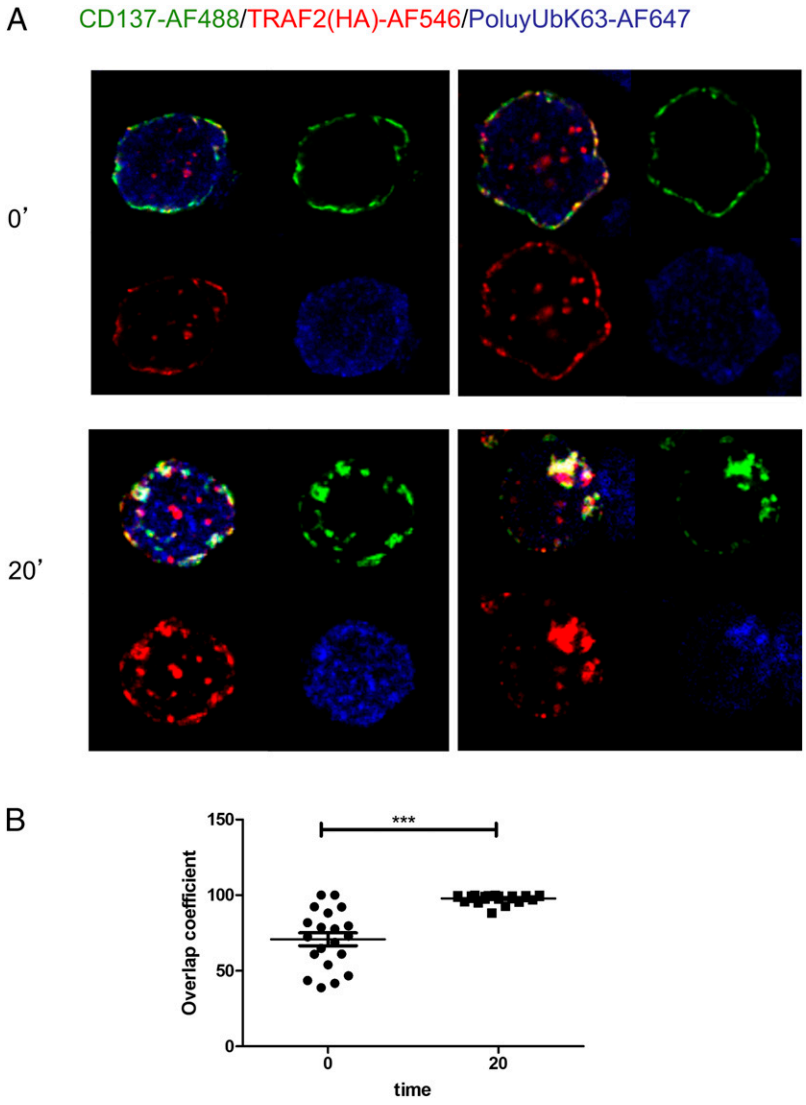

FIGURE 8. CD137, TRAF2, and K63–polyubiquitin (PolyubK63) codistribution. (**A**) HEK293T cells were transfected with CD137 (2.25 μg) and TRAF2-HA (2.25 μg) for 16 h. Cells were stimulated, and cross-linking was induced with biotinylated human anti-CD137 Ab (clone 6B4) and Alexa 488-streptavidin for the indicated time (0 and 20 min). After fixation (4% paraformaldehyde) and permeabilization (0.1% Triton X-100 in PBS), TRAF2 was stained with rat anti-HA mAb (1:400). K63-polyubiquitin chains (PolyubK63) were detected with clone Apu3 (1:40). Images were acquired with LSM 510 Zeiss confocal microscope (Zeiss) using 40× or 63× oil immersion objectives. For images shown, original magnification ×630. (**B**) Triple colocalization was quantified using a custom-developed FIJI plug-in that defines a mask in the green channel and calculates the colocalization coefficient of blue and red channels inside the mask. $***p < 0.0001$.

show a key role of K63 ubiquitination in CD137 endocytosis and also in CD137-mediated NF-κB induction. To assess the activity and signaling pathways triggered by the agonist anti-CD137 mAb in vivo, we have performed hydrodynamic injection of different combinations of expression plasmids encoding human CD137, a K63R ubiquitin mutant, and an NF-κB reporter system. This relatively easy in vivo technique takes advantage of the fact that hepatocytes efficiently take up all the coinjected expression cassettes. Hepatocytes will attain coexpression of all of the encoded proteins, thus allowing the study of the activity of the different Abs against CD137 in vivo in hepatocytes expressing CD137 and the different regulatory proteins. Our results clearly show that K63-linked polyubiquitination is required for efficient NF-κB induction in vivo triggered by anti-CD137 mAb as used in immunotherapy.

Elucidation of the downstream ubiquitination targets leading to NF-κB and MAPK activation would need additional biochemical studies. Unfortunately, the APU anti-K63–polyubiquitin Ab did not work in our hands for immunochemical studies such as immunoprecipitation, thus precluding a direct approach to identify K63-ubiquitinated polypeptides in response to CD137 activation. However, using pulldown experiments of cells transfected with plasmids encoding HA-tagged ubiquitin or its K48R and K63R mutants, we have shown that TRAF2 is specifically polyubiquitinated in K63 in response to CD137 engagement. This result is consistent with a role for TRAF2 in the regulation of CD137 signaling, as demonstrated by the significant inhibition, both in vivo and in vitro, of CD137-mediated NF-κB activation by enforced expression of a TRAF2 deletion mutant lacking the RING and zinc finger domains.

The involvement of TRAF2 and TRAF1 in the activation of NF-κB and MAPK by CD137 has been previously shown (37, 63). Our results illustrate that there exists a CD137 signaling pathway dependent on K63-linked polyubiquitination of substrates, including TRAF2, which is critical for CD137 biological functions. TRAF2 is considered an E3 ubiquitin ligase that uses armed Ubc13 as the E2 enzyme to catalyze K63-linked polyubiquitination (22, 23), and therefore, TRAF2 may self-ubiquitinate or be ubiquitinated by neighboring sister TRAF2 molecules. However, it is worth noting that recent structural data argue that TRAF2's RING domain might not interact with Ubc13 and other related E2 proteins and hence could not catalyze K63 polyubiquitination (64, 65). In this regard, TRAF2 also physically interacts with cIAP1 and -2, which are E3 ubiquitin ligases described to produce both K48– and K63–polyubiquitin chains (66, 67). Therefore, cIAP1 and/or -2 might be responsible for the CD137-induced K63 ubiquitination of TRAF2. However, we could not rule out the involvement of other TRAF family members, such as TRAF5, in this process (49).

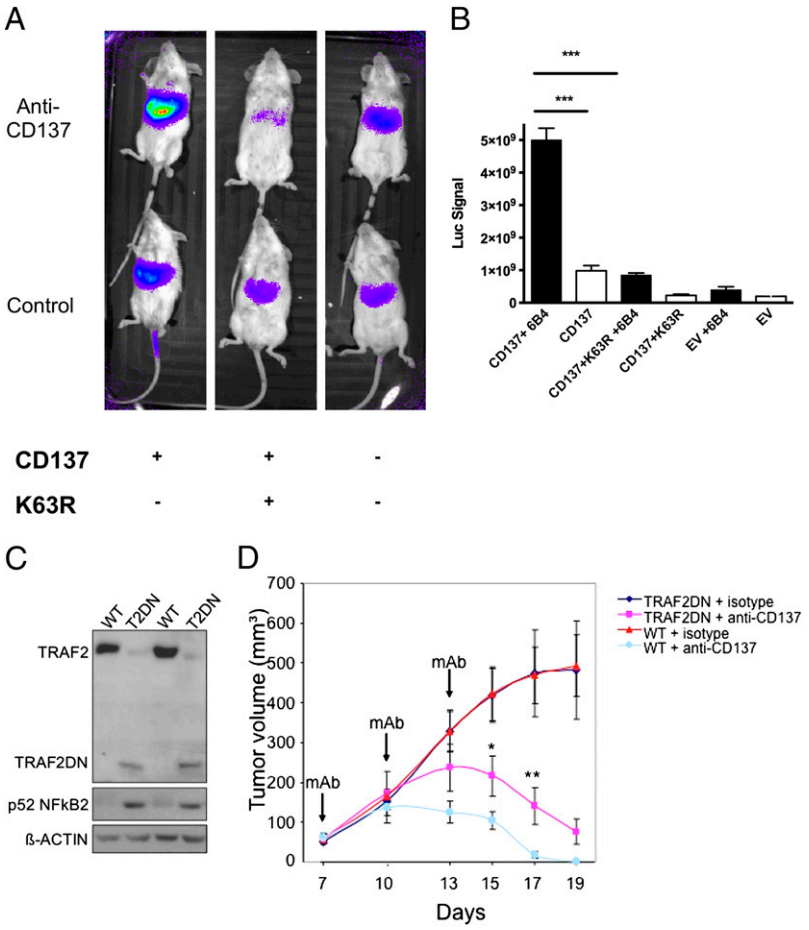

FIGURE 9. Triggering of NF-κB signaling by CD137 is dependent on K63 polyubiquitination, and TRAF2 is involved in efficient CD137-elicited tumor rejection in mice. (**A**) CD137-deficient mice were subjected to hydrodynamic gene transfer of the liver using plasmids encoding the same proteins detailed in Fig. 6 and a κB-firefly luciferase reporter. Forty-eight hours later, 100 μg 6B4 anti-CD137 mAb was i.p. administered. Bioluminescence measurements were performed 2 h after Ab injection. Data show representative images of liver luciferase expression after anti-CD137 mAb treatment. (**B**) Cumulative data for the experiments represented in (A). Data represent analyses of five mice per group. This set of experiments is representative of at least three similarly performed. (**C**) TRAF2 and p52 NF-κB protein content in T cells from WT and *Traf*2DN-tg (T2DN) mice. Each immunoblot lane represents one individual mouse of each genotype. (**D**) TRAF2 is required for efficient CD137-dependent tumor rejection in mice. *Traf*2DN-tg mice (♦ and ■) and WT littermates (▲ and ●) (6–8 wk old) were s.c. implanted with colon carcinoma CT26 cells and 7 d later were treated with 100 μg 1D8 anti-CD137 mAb (■ and ●) or isotype control (♦ and ▲). Treatment was repeated twice (3 and 6 d after the first treatment). Figure shows the volume of CT26 tumors at the indicated days. Statistical analysis shows mean ± SEM (n = 8/genotype and treatment condition). Unpaired t tests were used for statistical analysis of the effect of anti-CD137 mAb on tumor rejection. *p = 0.053, **p = 0.015, ***$p < 0.0001$. EV, Empty vector.

CD137-signaling pathways mediated by TRAF2 are important for T cell functions (63), and, according to our data, they are involved in eliciting efficient CD137-mediated antitumor immunity. Indeed, we have performed experiments in tg mice expressing in lymphocytes the TRAF2DN. Interestingly, in this mouse model, the expression of the TRAF2DN mutant in lymphocytes causes proteasome-dependent degradation of endogenous TRAF2, turning these *traf*2DN-tg mice into bona fide TRAF2-deficient mice (48) (Fig. 9C). Our results show that CT26 tumors s.c. implanted in the *Traf*2DN-tg mice were rejected as a result of anti-CD137 mAb treatment, although rejection was significantly delayed when compared with WT mice. However, it was surprising to observe that tumor rejection was still quite efficacious despite the virtual absence of TRAF2 in T lymphocytes. Furthermore, development of protective antitumor T cell memory was not significantly affected by the absence of TRAF2. These results suggest that the antitumor effect of CD137, at least under these therapeutic conditions, might also rely on other members of the TRAF family that might substitute TRAF2 in the tg T cells. As an alternative explanation, it is worth noting that NF-κB2 signaling pathways are deregulated in the *Traf*2DN-tg lymphocytes. Indeed, there is constitutive activation of the alternative NF-κB route as evidenced by p52 accumulation detected by Western blot on lysates from purified T cells (Fig. 9C). Constitutive alternative NF-κB activation might, at least partially, compensate for the reduced CD137-mediated canonical NF-κB induction as a result of TRAF2 deficiency. In any case, our results in the tg mice only link biologic activity(ies) of TRAF2 to CD137-triggered immunotherapy, but the role of K63-ubiquitination in this process remains to be determined.

All considered, CD137 in vivo internalization and K63–polyubiquitin signaling offer new perspectives for the study and development of CD137-based immunotherapy, as well as the search for much needed efficacy correlates and biomarkers.

Acknowledgments

We thank Dr. Lasarte for help with Biacore assays, Drs. Sandra Hervas-Stubbs, Tomás Aragón, Ainhoa Arina, Jesús Prieto (Centro de Investigación Médica Aplicada), Balbino Alarcon (Centro de Biología Molecular "Severo Ochoa," Madrid, Spain), Miguel A. del Pozo (Centro Nacional de Investigaciones Cardiovasculares, Madrid, Spain), Marco Gottardis (Bristol-Myers Squibb), Fernando Pastor (University of Miami, Miami, FL), Yongwon Choi (University of Pennsylvania, Philadelphia, PA), Adrian Ting, Gijs Veersteg, and Adolfo Garcia-Sastre (Mount Sinai School of Medicine), and Manuel S. Rodriguez (Fundación Instituto de Investigación Biomédica y Desarrollo Tecnológico, San Sebastian, Spain) for helpful discussions, collaborations, and/or reagents. We also thank Eneko Elizalde, Elena Ciordia, and Maria Gracia Gonzalez Bueno for continuous support at the animal facility of Centro de Investigación Médica Aplicada and Instituto de Investigaciones Biomedicas "Alberto Sols," Diego Alignani and Izaskun Gabari for technical support for cell sorting, and Miguel Larraga from the Centro de Investigación Médica Aplicada-Imaging Core Facility for developing the FIJI plugin used to quantify CD137, TRAF2, and K63 ubiquitin triple colocalization.

Disclosures

M.J.-K. is a full-time employee of Bristol-Myers Squibb. I.M. is a consultant for Bristol-Myers Squibb, AstraZeneca, Pfizer, and Digna Biotech. The other authors have no financial conflicts of interest.

References

1. Kwon, B. S., and S. M. Weissman. 1989. cDNA sequences of two inducible T-cell genes. *Proc. Natl. Acad. Sci. USA* 86: 1963–1967.
2. DeBenedette, M. A., N. R. Chu, K. E. Pollok, J. Hurtado, W. F. Wade, B. S. Kwon, and T. H. Watts. 1995. Role of 4-1BB ligand in costimulation of T lymphocyte growth and its upregulation on M12 B lymphomas by cAMP. *J. Exp. Med.* 181: 985–992.
3. Bertram, E. M., P. Lau, and T. H. Watts. 2002. Temporal segregation of 4-1BB versus CD28-mediated costimulation: 4-1BB ligand influences T cell numbers late in the primary response and regulates the size of the T cell memory response following influenza infection. *J. Immunol.* 168: 3777–3785.
4. Melero, I., J. V. Johnston, W. W. Shufford, R. S. Mittler, and L. Chen. 1998. NK1.1 cells express 4-1BB (CDw137) costimulatory molecule and are required for tumor immunity elicited by anti-4-1BB monoclonal antibodies. *Cell. Immunol.* 190: 167–172.
5. Wilcox, R. A., A. I. Chapoval, K. S. Gorski, M. Otsuji, T. Shin, D. B. Flies, K. Tamada, R. S. Mittler, H. Tsuchiya, D. M. Pardoll, and L. Chen. 2002. Cutting edge: Expression of functional CD137 receptor by dendritic cells. *J. Immunol.* 168: 4262–4267.
6. Pollok, K. E., Y. J. Kim, J. Hurtado, Z. Zhou, K. K. Kim, and B. S. Kwon. 1994. 4-1BB T-cell antigen binds to mature B cells and macrophages, and costimulates anti-mu-primed splenic B cells. *Eur. J. Immunol.* 24: 367–374.
7. Nishimoto, H., S. W. Lee, H. Hong, K. G. Potter, M. Maeda-Yamamoto, T. Kinoshita, Y. Kawakami, R. S. Mittler, B. S. Kwon, C. F. Ware, et al. 2005. Costimulation of mast cells by 4-1BB, a member of the tumor necrosis factor receptor superfamily, with the high-affinity IgE receptor. *Blood* 106: 4241–4248.
8. Palazón, A., A. Teijeira, I. Martínez-Forero, S. Hervás-Stubbs, C. Roncal, I. Peñuelas, J. Dubrot, A. Morales-Kastresana, J. L. Pérez-Gracia, M. C. Ochoa, et al. 2011. Agonist anti-CD137 mAb act on tumor endothelial cells to enhance recruitment of activated T lymphocytes. *Cancer Res.* 71: 801–811.
9. Olofsson, P. S., L. A. Söderström, D. Wågsäter, Y. Sheikine, P. Ocaya, F. Lang, C. Rabu, L. Chen, M. Rudling, P. Aukrust, et al. 2008. CD137 is expressed in human atherosclerosis and promotes development of plaque inflammation in hypercholesterolemic mice. *Circulation* 117: 1292–1301.
10. Broll, K., G. Richter, S. Pauly, F. Hofstaedter, and H. Schwarz. 2001. CD137 expression in tumor vessel walls. High correlation with malignant tumors. *Am. J. Clin. Pathol.* 115: 543–549.
11. Melero, I., W. W. Shuford, S. A. Newby, A. Aruffo, J. A. Ledbetter, K. E. Hellström, R. S. Mittler, and L. Chen. 1997. Monoclonal antibodies against the 4-1BB T-cell activation molecule eradicate established tumors. *Nat. Med.* 3: 682–685.
12. Tirapu, I., A. Arina, G. Mazzolini, M. Duarte, C. Alfaro, E. Feijoo, C. Qian, L. Chen, J. Prieto, and I. Melero. 2004. Improving efficacy of interleukin-12-transfected dendritic cells injected into murine colon cancer with anti-CD137 monoclonal antibodies and alloantigens. *Int. J. Cancer* 110: 51–60.
13. Melero, I., S. Hervas-Stubbs, M. Glennie, D. M. Pardoll, and L. Chen. 2007. Immunostimulatory monoclonal antibodies for cancer therapy. *Nat. Rev. Cancer* 7: 95–106.
14. Ito, F., Q. Li, A. B. Shreiner, R. Okuyama, M. N. Jure-Kunkel, S. Teitz-Tennenbaum, and A. E. Chang. 2004. Anti-CD137 monoclonal antibody administration augments the antitumor efficacy of dendritic cell-based vaccines. *Cancer Res.* 64: 8411–8419.
15. May, K. F., Jr., L. Chen, P. Zheng, and Y. Liu. 2002. Anti-4-1BB monoclonal antibody enhances rejection of large tumor burden by promoting survival but not clonal expansion of tumor-specific CD8+ T cells. *Cancer Res.* 62: 3459–3465.
16. Curran, M. A., M. Kim, W. Montalvo, A. Al-Shamkhani, and J. P. Allison. 2011. Combination CTLA-4 blockade and 4-1BB activation enhances tumor rejection by increasing T-cell infiltration, proliferation, and cytokine production. *PLoS ONE* 6: e19499.
17. Ascierto, P. A., E. Simeone, M. Sznol, Y. X. Fu, and I. Melero. 2010. Clinical experiences with anti-CD137 and anti-PD1 therapeutic antibodies. *Semin. Oncol.* 37: 508–516.
18. Fisher, T. S., C. Kamperschroer, T. Oliphant, V. A. Love, P. D. Lira, R. Doyonnas, S. Bergqvist, S. M. Baxi, A. Rohner, A. C. Shen, et al. 2012. Targeting of 4-1BB by monoclonal antibody PF-05082566 enhances T-cell function and promotes anti-tumor activity. *Cancer Immunol. Immunother.* 61: 1721–1733.
19. Arch, R. H., and C. B. Thompson. 1998. 4-1BB and Ox40 are members of a tumor necrosis factor (TNF)-nerve growth factor receptor subfamily that bind TNF receptor-associated factors and activate nuclear factor kappaB. *Mol. Cell. Biol.* 18: 558–565.
20. Jang, I. K., Z. H. Lee, Y. J. Kim, S. H. Kim, and B. S. Kwon. 1998. Human 4-1BB (CD137) signals are mediated by TRAF2 and activate nuclear factor-kappa B. *Biochem. Biophys. Res. Commun.* 242: 613–620.
21. Saoulli, K., S. Y. Lee, J. L. Cannons, W. C. Yeh, A. Santana, M. D. Goldstein, N. Bangia, M. A. DeBenedette, T. W. Mak, Y. Choi, and T. H. Watts. 1998. CD28-independent, TRAF2-dependent costimulation of resting T cells by 4-1BB ligand. *J. Exp. Med.* 187: 1849–1862.
22. Chen, Z. J. 2005. Ubiquitin signalling in the NF-kappaB pathway. *Nat. Cell Biol.* 7: 758–765.
23. Fukushima, T., S. Matsuzawa, C. L. Kress, J. M. Bruey, M. Krajewska, S. Lefebvre, J. M. Zapata, Z. Ronai, and J. C. Reed. 2007. Ubiquitin-conjugating enzyme Ubc13 is a critical component of TNF receptor-associated factor (TRAF)-mediated inflammatory responses. *Proc. Natl. Acad. Sci. USA* 104: 6371–6376.
24. Pineda, G., C. K. Ea, and Z. J. Chen. 2007. Ubiquitination and TRAF signaling. *Adv. Exp. Med. Biol.* 597: 80–92.
25. Chen, Z. J., L. Parent, and T. Maniatis. 1996. Site-specific phosphorylation of IkappaBalpha by a novel ubiquitination-dependent protein kinase activity. *Cell* 84: 853–862.
26. Karin, M., and E. Gallagher. 2009. TNFR signaling: ubiquitin-conjugated TRAFfic signals control stop-and-go for MAPK signaling complexes. *Immunol. Rev.* 228: 225–240.
27. Zhang, J., B. Stirling, S. T. Temmerman, C. A. Ma, I. J. Fuss, J. M. Derry, and A. Jain. 2006. Impaired regulation of NF-kappaB and increased susceptibility to colitis-associated tumorigenesis in CYLD-deficient mice. *J. Clin. Invest.* 116: 3042–3049.
28. Chiang, Y. J., H. K. Kole, K. Brown, M. Naramura, S. Fukuhara, R. J. Hu, I. K. Jang, J. S. Gutkind, E. Shevach, and H. Gu. 2000. Cbl-b regulates the CD28 dependence of T-cell activation. *Nature* 403: 216–220.
29. Lee, S. Y., A. Reichlin, A. Santana, K. A. Sokol, M. C. Nussenzweig, and Y. Choi. 1997. TRAF2 is essential for JNK but not NF-kappaB activation and regulates lymphocyte proliferation and survival. *Immunity* 7: 703–713.
30. Murillo, O., J. Dubrot, A. Palazón, A. Arina, A. Azpilikueta, C. Alfaro, S. Solano, M. C. Ochoa, C. Berasain, I. Gabari, et al. 2009. In vivo depletion of DC impairs the anti-tumor effect of agonistic anti-CD137 mAb. *Eur. J. Immunol.* 39: 2424–2436.
31. Wang, X., M. Li, H. Zheng, T. Muster, P. Palese, A. A. Beg, and A. García-Sastre. 2000. Influenza A virus NS1 protein prevents activation of NF-kappaB and induction of alpha/beta interferon. *J. Virol.* 74: 11566–11573.
32. Chadee, D. N., T. Yuasa, and J. M. Kyriakis. 2002. Direct activation of mitogen-activated protein kinase kinase kinase MEKK1 by the Ste20p homologue GCK and the adapter protein TRAF2. *Mol. Cell. Biol.* 22: 737–749.
33. O'Donnell, M. A., D. Legarda-Addison, P. Skountzos, W. C. Yeh, and A. T. Ting. 2007. Ubiquitination of RIP1 regulates an NF-kappaB-independent cell-death switch in TNF signaling. *Curr. Biol.* 17: 418–424.
34. Newton, K., M. L. Matsumoto, I. E. Wertz, D. S. Kirkpatrick, J. R. Lill, J. Tan, D. Dugger, N. Gordon, S. S. Sidhu, F. A. Fellouse, et al. 2008. Ubiquitin chain editing revealed by polyubiquitin linkage-specific antibodies. *Cell* 134: 668–678.
35. Schindelin, J., I. Arganda-Carreras, E. Frise, V. Kaynig, M. Longair, T. Pietzsch, S. Preibisch, C. Rueden, S. Saalfeld, B. Schmid, et al. 2012. Fiji: an open-source platform for biological-image analysis. *Nat. Methods* 9: 676–682.
36. Arina, A., O. Murillo, J. Dubrot, A. Azpilikueta, I. Gabari, J. L. Perez-Gracia, C. Alfaro, C. Berasain, J. Prieto, S. Ferrini, et al. 2008. Interleukin-15 liver gene transfer increases the number and function of IKDCs and NK cells. *Gene Ther.* 15: 473–483.
37. McPherson, A. J., L. M. Snell, T. W. Mak, and T. H. Watts. 2012. Opposing roles for TRAF1 in the alternative versus classical NF-κB pathway in T cells. *J. Biol. Chem.* 287: 23010–23019.
38. Wang, C., A. J. McPherson, R. B. Jones, K. S. Kawamura, G. H. Lin, P. A. Lang, T. Ambagala, M. Pellegrini, T. Calzascia, N. Aidarus, et al. 2012. Loss of the signaling adaptor TRAF1 causes CD8+ T cell dysregulation during human and murine chronic infection. *J. Exp. Med.* 209: 77–91.
39. Vallabhapurapu, S., and M. Karin. 2009. Regulation and function of NF-kappaB transcription factors in the immune system. *Annu. Rev. Immunol.* 27: 693–733.
40. Bhoj, V. G., and Z. J. Chen. 2009. Ubiquitylation in innate and adaptive immunity. *Nature* 458: 430–437.
41. Alvarez, S. E., K. B. Harikumar, N. C. Hait, J. Allegood, G. M. Strub, E. Y. Kim, M. Maceyka, H. Jiang, C. Luo, T. Kordula, et al. 2010. Sphingosine-1-phosphate is a missing cofactor for the E3 ubiquitin ligase TRAF2. *Nature* 465: 1084–1088.
42. Matsuzawa, A., P. H. Tseng, S. Vallabhapurapu, J. L. Luo, W. Zhang, H. Wang, D. A. Vignali, E. Gallagher, and M. Karin. 2008. Essential cytoplasmic translocation of a cytokine receptor-assembled signaling complex. *Science* 321: 663–668.
43. Shembade, N., R. Pujari, N. S. Harhaj, D. W. Abbott, and E. W. Harhaj. 2011. The kinase IKKα inhibits activation of the transcription factor NF-κB by phosphorylating the regulatory molecule TAX1BP1. *Nat. Immunol.* 12: 834–843.
44. Barriere, H., C. Nemes, D. Lechardeur, M. Khan-Mohammad, K. Fruh, and G. L. Lukacs. 2006. Molecular basis of oligoubiquitin-dependent internalization of membrane proteins in Mammalian cells. *Traffic* 7: 282–297.
45. Marx, C., J. M. Held, B. W. Gibson, and C. C. Benz. 2010. ErbB2 trafficking and degradation associated with K48 and K63 polyubiquitination. *Cancer Res.* 70: 3709–3717.
46. Kumar, K. G., H. Barriere, C. J. Carbone, J. Liu, G. Swaminathan, P. Xu, Y. Li, D. P. Baker, J. Peng, G. L. Lukacs, and S. Y. Fuchs. 2007. Site-specific ubiquitination exposes a linear motif to promote interferon-alpha receptor endocytosis. *J. Cell Biol.* 179: 935–950.
47. Palazon, A., I. Martinez-Forero, A. Teijeira, A. Morales-Kastresana, C. Alfaro, M. F. Sanmamed, J. L. Perez-Gracia, I. Penuelas, S. Hervas-Stubbs, A. Rouzaut, et al. 2012. The HIF-1α hypoxia response in tumor-infiltrating T lymphocytes induces functional CD137 (4-1BB) for immunotherapy. *Cancer Discovery* 2: 608–623.
48. Pérez-Chacón, G., D. Llobet, C. Pardo, J. Pindado, Y. Choi, J. C. Reed, and J. M. Zapata. 2012. TNFR-associated factor 2 deficiency in B lymphocytes predisposes to chronic lymphocytic leukemia/small lymphocytic lymphoma in mice. *J. Immunol.* 189: 1053–1061.
49. Tada, K., T. Okazaki, S. Sakon, T. Kobarai, K. Kurosawa, S. Yamaoka, H. Hashimoto, T. W. Mak, H. Yagita, K. Okumura, et al. 2001. Critical roles of TRAF2 and TRAF5 in tumor necrosis factor-induced NF-kappa B activation and protection from cell death. *J. Biol. Chem.* 276: 36530–36534.
50. Fonsatti, E., M. Maio, M. Altomonte, and P. Hersey. 2010. Biology and clinical applications of CD40 in cancer treatment. *Semin. Oncol.* 37: 517–523.
51. Jensen, S. M., L. D. Maston, M. J. Gough, C. E. Ruby, W. L. Redmond, M. Crittenden, Y. Li, S. Puri, C. H. Poehlein, N. Morris, et al. 2010. Signaling through OX40 enhances antitumor immunity. *Semin. Oncol.* 37: 524–532.

52. Alcover, A., and B. Alarcón. 2000. Internalization and intracellular fate of TCR-CD3 complexes. *Crit. Rev. Immunol.* 20: 325–346.
53. Melero, I., O. Murillo, J. Dubrot, S. Hervás-Stubbs, and J. L. Perez-Gracia. 2008. Multi-layered action mechanisms of CD137 (4-1BB)-targeted immunotherapies. *Trends Pharmacol. Sci.* 29: 383–390.
54. van Schouwenburg, P. A., L. A. van de Stadt, R. N. de Jong, E. E. van Buren, S. Kruithof, E. de Groot, M. Hart, S. M. van Ham, T. Rispens, L. Aarden, et al. 2013. Adalimumab elicits a restricted anti-idiotypic antibody response in autoimmune patients resulting in functional neutralisation. *Ann. Rheum. Dis.* 72: 104–109.
55. Ye, Z., I. Hellström, M. Hayden-Ledbetter, A. Dahlin, J. A. Ledbetter, and K. E. Hellström. 2002. Gene therapy for cancer using single-chain Fv fragments specific for 4-1BB. *Nat. Med.* 8: 343–348.
56. Snell, L. M., G. H. Lin, A. J. McPherson, T. J. Moraes, and T. H. Watts. 2011. T-cell intrinsic effects of GITR and 4-1BB during viral infection and cancer immunotherapy. *Immunol. Rev.* 244: 197–217.
57. Croft, M. 2003. Co-stimulatory members of the TNFR family: keys to effective T-cell immunity? *Nat. Rev. Immunol.* 3: 609–620.
58. White, A. L., H. T. Chan, A. Roghanian, R. R. French, C. I. Mockridge, A. L. Tutt, S. V. Dixon, D. Ajona, J. S. Verbeek, A. Al-Shamkhani, et al. 2011. Interaction with FcγRIIB is critical for the agonistic activity of anti-CD40 monoclonal antibody. *J. Immunol.* 187: 1754–1763.
59. Li, F., and J. V. Ravetch. 2011. Inhibitory Fcγ receptor engagement drives adjuvant and anti-tumor activities of agonistic CD40 antibodies. *Science* 333: 1030–1034.
60. Kalos, M., B. L. Levine, D. L. Porter, S. Katz, S. A. Grupp, A. Bagg, and C. H. June. 2011. T cells with chimeric antigen receptors have potent antitumor effects and can establish memory in patients with advanced leukemia. *Sci. Transl. Med.* 3: 95ra73.
61. Porter, D. L., B. L. Levine, M. Kalos, A. Bagg, and C. H. June. 2011. Chimeric antigen receptor-modified T cells in chronic lymphoid leukemia. *N. Engl. J. Med.* 365: 725–733.
62. Stephan, M. T., V. Ponomarev, R. J. Brentjens, A. H. Chang, K. V. Dobrenkov, G. Heller, and M. Sadelain. 2007. T cell-encoded CD80 and 4-1BBL induce auto- and transcostimulation, resulting in potent tumor rejection. *Nat. Med.* 13: 1440–1449.
63. Cannons, J. L., E. M. Bertram, and T. H. Watts. 2002. Cutting edge: profound defect in T cell responses in TNF receptor-associated factor 2 dominant negative mice. *J. Immunol.* 169: 2828–2831.
64. Zheng, C., V. Kabaleeswaran, Y. Wang, G. Cheng, and H. Wu. 2010. Crystal structures of the TRAF2: cIAP2 and the TRAF1: TRAF2: cIAP2 complexes: affinity, specificity, and regulation. *Mol. Cell* 38: 101–113.
65. Yin, Q., B. Lamothe, B. G. Darnay, and H. Wu. 2009. Structural basis for the lack of E2 interaction in the RING domain of TRAF2. *Biochemistry* 48: 10558–10567.
66. Xu, M., B. Skaug, W. Zeng, and Z. J. Chen. 2009. A ubiquitin replacement strategy in human cells reveals distinct mechanisms of IKK activation by TNFalpha and IL-1beta. *Mol. Cell* 36: 302–314.
67. Labbé, K., C. R. McIntire, K. Doiron, P. M. Leblanc, and M. Saleh. 2011. Cellular inhibitors of apoptosis proteins cIAP1 and cIAP2 are required for efficient caspase-1 activation by the inflammasome. *Immunity* 35: 897–907.